Desalination and Water Treatment
www.deswater.com
doi: 10.5004/dwt.2020.26438

207 (2020) 287–299
December

Studies on removal of Cu(II) from aqueous solution by adsorption on fly ash agglomerates

Justyna Ulatowska*, Krzysztof Jan Legawiec, Jowita Drzyzga, Izabela Polowczyk

Department of Process Engineering and Technology of Polymers and Carbon Materials, Wroclaw University of Science and Technology, Wybrzeże Wyspiańskiego Street 27, Wrocław, Lower Silesia 50-370, Poland, emails: justyna.ulatowska@pwr.edu.pl (J. Ulatowska), krzysztof.legawiec@pwr.edu.pl (K.J. Legawiec), jowita.drzyzga@pwr.edu.pl (J. Drzyzga), izabela.polowczyk@pwr.edu.pl (I. Polowczyk)

Received 14 April 2020; Accepted 10 August 2020

ABSTRACT

The objective of the present study is to assess the efficiency of the fly ash agglomerates (particle size: 2.5–5.0 mm) concerning Cu(II) removal from aqueous solution. The experiments have been carried out by using fly ash from brown coal and biomass burning power plant Zgierz (Poland). The tumble agglomeration experiments have been conducted in the laboratory granulator. Adsorbent dosage contact time and initial Cu(II) concentration on the adsorption were investigated. The maximum adsorption capacity achieved for fly ash agglomerates is 43.82 mg Cu(II)/g for 10 g/dm^3 adsorbent-to-solute ratio. For 1,000 mg/dm^3 Cu(II) solution the maximum removal was about 99% for 225 g/dm^3 adsorbent-to-solute ratio. The adsorption kinetics experimental data were fitted well with the pseudo-second-order model. An intra-particle diffusion model was examined. The Freundlich isotherm model is more adequate than the Langmuir or Dubinin–Radushkevich one while fitting the adsorption results of Cu(II) onto fly ash agglomerates at 25°C. Column studies data were evaluated by using Thomas and Yoon–Nelson models. Fly ash agglomerates can be effective, low-cost, and easy-handling adsorbent for the removal of toxic Cu(II) ions from aqueous solution both in batch and column processes. To complement Cu(II) adsorption study was made FT-IR spectra.

Keywords: Copper(II) ion; Adsorption isotherm studies; Adsorption kinetics; Column study

1. Introduction

Anthropopressure is a total of human activities which, in effect, transform the natural environment. The effect of the processes performed in the production plants is the emission of various types of pollutants, which, despite the development of wastewater treatment techniques, are released into surface waters and the atmosphere. One of the most important challenges for the industry is to reduce the realizing of heavy metals to water, soil, and air due to their hazardous effects on humans and ecosystems. Moreover, these contaminants come mainly from the metallurgical and mining industries [1–3]. Within the numerous heavy metal ions in industrial wastewater, anionic, and soluble form of copper in the double-positive cation type can be found. Exposure of living organisms to an excess of ionic Cu forms can lead to serious health problems, which has been extensively described in the literature [4–6], even though copper is needed by organisms for enzyme synthesis and tissue development [7].

Recent works on the treatment of wastewater in fixed-bed columns focus on adsorption onto various types of materials [8,9]. If the adsorbent is a waste material, such as activated carbon [10,11] and fly ash [12–14], it can be considered as cost-effective and contribute to sustainable development. Fly ash is generated during coal or biomass combustion processes. The amounts of such industrial waste generated in thermal energy production operations are quite significant

* Corresponding author.

and pose a relevant problem for power plants. This problem is particularly noticeable in Poland, where 72.4% of electricity is produced from hard coal and lignite. Consequently, as much as 294 million tons of fly ash is generated annually (according to the statistical yearbook of the Polish Central Statistical Office). The present directions of its utilization have been aimed at use as a building material, filler, and soil amendment that may improve physical, chemical, and biological properties of the degraded soils and as a source of readily available plant micro- and macro-nutrients [15,16]. Fly ash has a highly alkaline nature, which predisposes it to adsorption of heavy metal ions, for example, As, Cd, Cu, and Tl [17–22], as well as boron removal [23,24] and organic dyes [25,26]. In industrial applications, fly ash is converted into a more practical form of briquettes, granules, and pellets [27,28]. A variety of adsorbents, including natural materials, modified natural materials, industrial by-products, nanomaterials, and low-cost biosorbent have been used for copper removal [1,4,5,8–14,29–35].

This study aims to investigate Cu(II) removal from aqueous solution by fly ash agglomerates and to suggest a possible solution for waste disposal. Both batch and column adsorption of Cu(II) experiments were conducted. The application of this simple adsorption-based method is promising in regions where water treatment is highly challenging, especially where other technologies, such as coagulation, membrane filtration, or biological treatment is impossible [4].

2. Materials and methods

2.1. Fly ash

Fly ash used in these studies makes from lignite and biomass-burning power plant Zgierz (Poland). The characteristics of the material were presented in Polowczyk et al.s' [27] paper. Fly ash used in this study consisted of anhydrite (44.2%), quartz (29.5%), calcium oxide (16.9%), unburned carbon (5.5%), calcite (2.4%), and hematite (1.5%). In Fig. 1, scanning electron microscopy (SEM) micrographs morphology of fly ash can be recognized. The density of fly ash is as 2.70 g/cm^3 and it was determined using a pycnometer. The surface area of fly ash is 17.3 m^2/g and was measured with the BET/N_2 (Brunauer–Emmett–Teller) method. Particle size analysis showed a volume median diameter (d50) of about 105.5 μm, while d10 and d90 are 17.8 and 212.6 μm, respectively, and the particle analysis was carried out using a Mastersizer 2000 laser diffractometer (Malvern, UK), equipped with a HydroMu dispersion unit (Malvern, UK). The median (d50) is the diameter where half of the sizes are smaller than this value and half are larger. The d10 diameter has ten percent smaller and ninety percent larger and d90 describes the diameter where ninety percent of the distribution has a smaller particle size and 10% has a larger particle size.

2.2. Agglomeration process

The tumble agglomeration of fly ash has been conducted in a laboratory disc granulator. Fly ash was continuously fed onto an inclined 45°, rotating dish granulator (dish diameter 400 mm) driven by a motor at 150 rpm. Water was used as a binder liquid. The liquid was atomized over the powder by compressed air at a volumetric flow rate of 11 cm^3/min. In each experiment, 1,000 g of fly ash samples were taken, and the agglomeration process was carried out for 45 min. After this time, the agglomerates were formed. The wet product was cured for 1 week to release hydration of cementitious components at ambient temperature (25°C) and then dried. After that, the agglomerates were divided into several fractions. For the adsorption study, the fraction of 2.5–5.0 mm was used. The specific surface area of agglomerates equals 25.9 m^2/g. Compared to the fly ash specific surface area, this value is higher, which is related to the formation of C–S–H

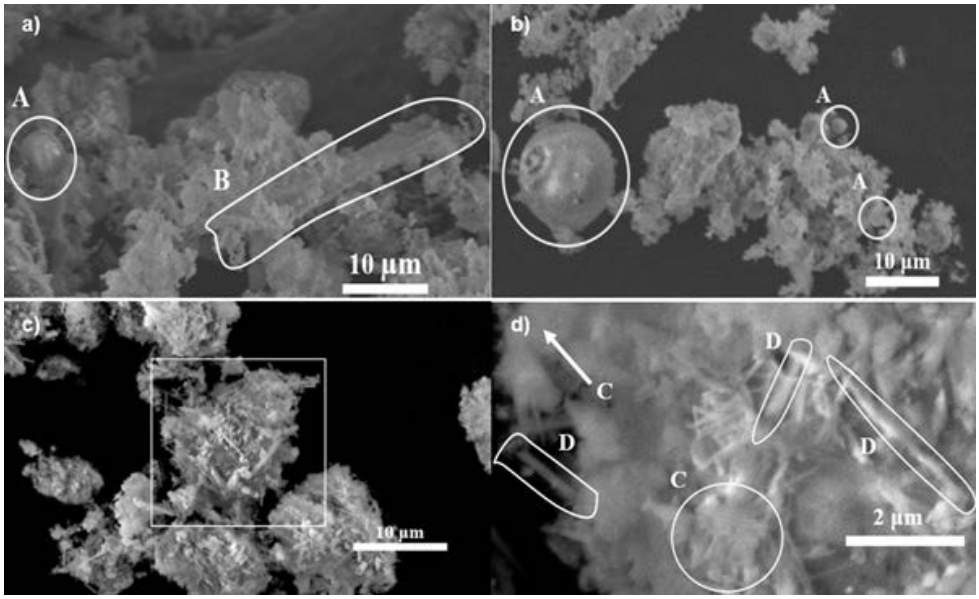

Fig. 1. SEM micrographs of fly ash sample (a and b) and fly ash agglomerates (c and d): A – spherical grains of microspheres; B – elongated anhydrite crystals, C – C-S-H phase, D – ettringite structures.

and ettringite phase. Differences in a crystalline composition are shown in Fig. 1 and were discussed in Polowczyk et al.'s [27] paper. The mechanic strength analysis of agglomerates was investigated by the monoaxial compression method using a compact tabletop testing machine EZ Test LX (Shimadzu, Japan) equipped with 500 N load cell (Shimadzu, Japan). The destructive force was determined by placing the agglomerate on a jig platform and slowly lowering the compression plate (rate of descent – 5 mm/min) until the sample cracks. The 10 compression test resulted in an average maximum force of 7.24 N with a standard deviation of ±0.91 N.

2.3. Adsorption experiments

All chemicals used in the present work were of analytical purity. The stock solution of Cu(II) was prepared in 1.0 g/dm^3 concentration using $CuSO_4 \cdot 5H_2O$ and then diluted to appropriate concentrations for each test.

Adsorption of Cu(II) from aqueous solutions was investigated in batch and column experiments. Cu(II) concentration in solution was analyzed by using a laboratory ion meter (CPI-505 ELMERON), equipped with an ion-selective electrode with a solid–copper membrane (Ecu-01 HYDROMET) and with a reference electrode (EAgCIP-311T EUROSENSOR). The experimental setup for analyzing of Cu(II) is shown in Fig. 2.

The experiments of Cu(II) adsorption from aqueous solution was carried out on the fly ash agglomerates of the diameter between 2.5 and 5.0 mm. The image of fly ash agglomerates is shown in Fig. 3. Different of fly ash agglomerates amounts (0.1–2.25 g) was applied to 10 cm^3 of the solution containing 500 mg/dm^3 or 1,000 mg/dm^3 Cu(II) solution to find out the effect of adsorbent dosage on Cu(II) removal. In a kinetic study, the batch experiment was repeated at different time intervals using 0.5 g of adsorbents and 10 cm^3 of the solution containing 1,000 mg/dm^3 Cu(II) solution. Cu(II) concentration was monitored for 24 h, starting at the second minute. The measurements were carried out at 2, 5 10, 15, 30, 60, 120, 240, 480, and 1,440 min. Isotherm studies were performed by varying the initial Cu(II) concentrations (25–1,000 mg/dm^3), keeping the adsorbent dose of 0.5 g. The resulting suspensions were shaken for 24 h. All experiments were carried out at 25°C ± 1°C. The amount of adsorption (q) was calculated by the following equation [12,13]:

$$q = \frac{\left[\left(c_0 - c_{eq}\right) \cdot V\right]}{m} \quad (1)$$

where c_0 and c_{eq} (mg/g) are the initial and equilibrium Cu(II) concentrations, respectively. V (cm^3) is the volume of the solution, and m (g) is the amount of adsorbent used.

All the experiments with adsorption of Cu(II) were carried out at pH around 5.50 because the real wastewater containing copper ions have acidic pH.

These experiments were performed in a small-scale cylindrical fixed-bed column (1.5 cm internal diameter and 15 cm length). The column was packed with fly ash agglomerates on glass wool support. The bed height was 10 cm, and the corresponding bed was loaded with 10 g of fly ash agglomerates. Cu(II) solution (500 mg/dm^3) at natural pH was delivered downflow to the column using a peristaltic pump (ZALIMP 315) at a 1.5 cm^3/min flow rate. All the column studies were performed at room temperature of 25°C ± 1°C. Samples were collected at certain time intervals and then analyzed for remaining Cu(II) concentration. The column experiments were continued until a constant Cu(II) concentration was obtained in the effluent. All experiments have been made in duplicate. The experimental setup is given in Fig. 3.

After column adsorption experiments, the fly ash agglomerates were separated in a sieve and air-dried, then 500 cm^3 of distilled water was added for 48 h and shaken to check that Cu(II) is permanently bound to the adsorbent.

2.4. Adsorption modeling approaches

2.4.1. Kinetic models of adsorption

2.4.1.1. Elovich model

One of the most useful models for describing adsorption is the Elovich equation [36,37], which is given by:

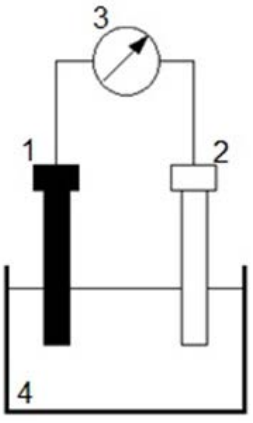

Fig. 2. The experimental setup for analyzing of Cu(II) (1 – the ion-selective electrode with a solid-copper membrane; 2 – the reference electrode; 3 – the laboratory ion meter; 4 – the aqueous solution).

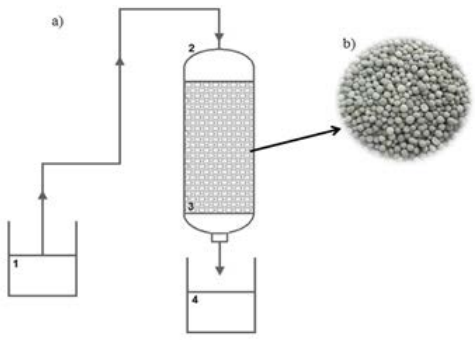

Fig. 3. (a) The experimental setup for adsorption of Cu(II) from aqueous solution: 1 – influent (stock solution of Cu(II): 500 mg/dm^3), 2 – glass column, 3 – fixed bed, 4 – effluent; (b) fly ash agglomerates: fraction 2.5–5.0 mm.

$$q = q_0 + \left[\frac{1}{\beta}\cdot\ln(\alpha\cdot\beta)\right] + \left[\frac{1}{\beta}\cdot\ln(t)\right] \quad (2)$$

where α (g min²/mg) is the initial sorption rate, the parameter β (mg/g min) is related to the extent of surface coverage and activation energy of chemisorption, and $q = q_0$ at $t = 0$.

2.4.1.2. Pseudo-first-order model

The pseudo-first-order (PFO) equation (Lagergren's equation) describes adsorption in solid–liquid systems based on the sorption capacity of solids, and this model is given as follows [38]:

$$\frac{dQ_1}{dt} = k_1(Q_1 - q_t) \quad (3)$$

After integration with the initial condition $q_t = 0$ at $t = 0$, can be obtained.

$$q_t = Q_1\left[1 - \exp(-k_1\cdot t)\right] \quad (4)$$

where q_t (mg/g) is the adsorption capacity at time t (min), Q_1 (mg/g) the amount of adsorption equilibrium, and k_1 (1/min) is the rate constant of the PFO adsorption. The rate constant, k_1, and correlation coefficients (R^2) were calculated from the linear plots of $\log(Q_1 - q_t)$ vs. t.

2.4.1.3. Pseudo-second-order model

The pseudo-second-order (PSO) rate expression, which has been applied for analyzing chemisorption kinetics from liquid solutions [39]. This model is given in the following form:

$$\frac{dQ_2}{dt} = k_2^2\cdot(Q_2 - q_t)^2 \quad (5)$$

When the initial condition is $q_t = 0$ at $t = 0$, after integration:

$$q_t = \frac{k_2\cdot Q_2^2\cdot t}{(1 + k_2\cdot Q_2\cdot t)} \quad (6)$$

It can be represented in a linear expression from the linear plots of t/q_t as:

$$\frac{t}{q_t} = \frac{1}{(k_2\cdot Q_2^2)} + \frac{t}{q_t} \quad (7)$$

where k_2 (g/mg min) is the rate constant of the PSO equation, Q_2 (mg/g) is the amount of adsorption equilibrium and q_t (mg/g) is the amount of adsorption at any time t (min). $k_2Q_2^2 = h$ denotes the initial adsorption rate (mg/g min). This model is more likely to predict the kinetic behavior of adsorption with chemical sorption being the rate-controlling step [39].

The slowest step of adsorption, that is, the rate-limiting step may perform by either the boundary layer (film) or as the intra-particle (pore) diffusion. The intra-particle diffusion model is given as follows [13,37]:

$$q_t = k_{IP}\cdot t^{0.5} + b \quad (8)$$

where q_{eq} (mg/g) is the adsorption capacity at any time t (min), and k_{IP} (mg/g min$^{1/2}$) is the intra-particle diffusion model rate constant, and b (mg/g) is the film thickness.

The higher the value of b, the greater the effect of the boundary layer on the adsorption process. If the rate-limiting step is the intra-particle diffusion, the plot of q_t vs. $t^{1/2}$ should be a straight line. The variation of the plot from the linearity suggests that the rate-limiting step should be the boundary layer (film) diffusion-controlled [13].

2.4.2. Equilibrium isotherms

The adsorption isotherm evaluation is crucial to determine the adsorption capacity and to analyze the adsorption mechanism. Usually, Freundlich and Langmuir adsorption isotherm models are used to determining the adsorption equilibrium and fit the experimental data of heavy metal ions adsorption. In this work, the experimental data of Cu(II) adsorption were described using with Freundlich, Langmuir, and Dubinin–Radushkevich equations. The isotherm parameters were obtained with linear regression. Table 1 shows isotherm models and their linearized forms applied in the present work.

2.4.2.1. Freundlich model

The Freundlich equation is an empirical expression based on adsorption on a heterogeneous surface. The Freundlich model is represented by the equation [40]:

$$q_{eq} = K_F\cdot C_{eq}^{(1/n)} \quad (9)$$

where K_F (mg/g) is Freundlich constant related to the adsorption capacity of adsorbent and n (dimensionless) is a Freundlich exponent indicating the adsorption intensity.

2.4.2.2. Langmuir model

The Langmuir isotherm model has been successfully applied to many adsorption processes, and the basic Langmuir theory is that adsorption takes place at specific homogeneous sites within the adsorbent. The Langmuir equation is [41]:

$$q_{eq} = \frac{Q_L K_L\cdot c_{eq}}{(1 + K_L\cdot c_{eq})} \quad (10)$$

where q_{eq} and Q_L are the equilibrium and monolayer adsorption capacities of the adsorbent (mg/g), respectively, c_{eq} is the equilibrium Cu(II) concentration in the solution (mg/dm³), and K_L is the Langmuir constant (dm³/g) related to the free energy of adsorption.

Four linearized forms of Langmuir equations are presented in Table 1. The parameters of Langmuir isotherm

Table 1
Linear and non-linear isotherm equations

Isotherm	Equation	Linear form	Relationship
Freundlich	$q_{eq} = K_F \cdot c_{eq}^{1/n}$	$\log(q_{eq}) = \log(K_F) + \frac{1}{n} \cdot \log(c_{eq})$	$\log(q_{eq})$ vs. $\log(c_{eq})$
Langmuir-I	$q_{eq} = \frac{Q_L \cdot K_L \cdot c_{eq}}{(1 + K_L \cdot c_{eq})}$	$\frac{c_{eq}}{q_{eq}} = \left[\frac{1}{(Q_L \cdot K_L)}\right] + \frac{c_{eq}}{Q_L}$	$\frac{c_{eq}}{q_{eq}}$ vs. $\frac{1}{c_{eq}}$
Langmuir-II		$\frac{1}{q_{eq}} = \left[\frac{1}{(Q_L \cdot K_L)}\right] \cdot \frac{1}{c_{eq}} + \frac{1}{Q_L}$	$\frac{1}{q_{eq}}$ vs. $\frac{1}{c_{eq}}$
Langmuir-III		$q_{eq} = Q_L - \left[\frac{1}{K_L}\right] \cdot \frac{q_{eq}}{c_{eq}}$	q_{eq} vs. $\frac{q_{eq}}{c_{eq}}$
Langmuir-IV		$\frac{q_{eq}}{c_{eq}} = K_L \cdot Q_L - K_L \cdot q_{eq}$	$\frac{q_{eq}}{c_{eq}}$ vs. q_{eq}
Dubinin–Radushkevich	$q_{eq} = Q_{DR} \cdot \exp(-k_{DR} \cdot \varepsilon^2)$	$\ln(q_{eq}) = \ln(Q_{DR}) - K_{DR} \cdot \varepsilon^2$	$\ln(q_{eq})$ vs. ε^2

equations were determined by plotting graphs between c_{eq}/q_{eq} vs. c_{eq} (Langmuir-I), $1/q_{eq}$ vs. $1/c_{eq}$ (Langmuir-II), q_{eq} vs. q_{eq}/c_{eq} (Langmuir-III), and q_{eq}/c_{eq} vs. q_{eq} (Langmuir-IV) [42].

2.4.2.3. Dubinin–Radushkevich model

Since the Freundlich and Langmuir isotherm models do not give any idea about the mechanism of adsorption, the equilibrium data are tested with the Dubinin–Radushkevich (D–R). Dubinin and Radushkevich have reported that the characteristic adsorption curve is related to the porous structure of a sorbent. D–R equation is generally expressed as follows [43]:

$$\ln(q_{eq}) = \ln(Q_{DR}) - k_{DR} \cdot \varepsilon^2 \tag{11}$$

where ε is the RT ln(1 + 1/c_{eq}) (Polanyi potential). Q_{DR} (mg/g) is the theoretical saturation capacity, k_{DR} (mol^2/kJ^2) is the constant related to the adsorption energy, R is the gas constant (8.314 kJ/mol), and T is the absolute temperature (K). The D–R isotherm is used to determine if the adsorption process is chemical or physical in nature. The low free energy of adsorption (E) can be calculated from the k_{DR} value using the following relation [43]:

$$E = \frac{1}{\left[(2 \cdot k_{DR})^{1/2}\right]} \tag{12}$$

2.4.3. Column studies

Adsorption in a fixed bed can be described by using two most common models: the Thomas model and the Yoon–Nelson model. Table 2 shows the equations of these models and their linear forms.

2.4.3.1. Thomas model

The Thomas model is one of the overall and widely used to describe the performance theory of the adsorption process in a fixed-bed column. This model is appropriate in a laboratory system with a constant flow rate and non-axial dispersion and is behavior matches the Langmuir isotherm [41]. The equation is the following [44,45]:

$$\ln\left[\left(\frac{c_0}{c_t}\right) - 1\right] = \left(\frac{k_{Th} \cdot q_{Th}}{Q}\right) - \left(\frac{k_{Th} \cdot c_0 \cdot V}{Q}\right) \tag{13}$$

where c_0 and c_t are the initial and effluent concentration (mg/dm^3), respectively, k_{Th} is the Thomas rate constant (cm^3/mg min), Q is the volumetric flow rate (dm^3/min), and m is the amount of adsorbent in the column (g). The constant kinetic k_{Th} and the adsorption capacity of the column q_{Th} can be calculated from a plot of ln((c_0/c_t) – 1) vs. V according to Eq. (13).

2.4.3.2. Yoon–Nelson model

The Yoon–Nelson model is a straightforward and transparent model, which does not demand any information related to the property of adsorbate, adsorbent type, and the physical property of the adsorption bed [46]. The linearized form of Yoon–Nelson model for a single component system is expressed as [46]:

$$\ln\left[\frac{c_t}{(c_0 - c_t)}\right] = k_{YN}(t - \tau) \tag{14}$$

where k_{YN} is the rate constant (1/min) and τ is the time required for 50% adsorbate breakthrough (min). The values of parameters k_{YN} and τ for the adsorbate can be calculated from the plot of ln($c_t/(c_0 - c_t)$) vs. time (t) according to Eq. (14).

Table 2
Mathematical equations and breakthrough curves equations of used models

Model	Mathematical equation	Linear dependence	Breakthrough curve
Thomas	$\ln\left[\left(\frac{c_0}{c_t}\right)-1\right]=\left(\frac{k_{Th}\cdot q_{Th}}{Q}\right)-\left(\frac{k_{Th}\cdot c_0}{Q}\right)V$	$\ln\left[\left(\frac{c_0}{c_t}\right)-1\right]$ vs. V	$\frac{c_t}{c_0}=\frac{1}{\left\{1+\exp\left[\left(k_{Th}/Q\right)\left(q_{Th}\cdot m-c_0\cdot V\right)\right]\right\}}$
Yoon-Nelson	$\ln\left[\frac{c_t}{\left(c_0-c_t\right)}\right]=k_{YN}\cdot\left(t-\tau\right)$	$\ln\left[\frac{c_t}{\left(c_0-c_t\right)}\right]$ vs. t	$\frac{c_t}{c_0}=\frac{c_0\cdot\exp\left[k_{YN}\cdot\left(t-\tau\right)\right]}{\left\{1+\exp\left[k_{YN}\cdot\left(t-\tau\right)\right]\cdot c_0\right\}}$

3. Results and discussion

3.1. Effect of adsorbent dose

Adsorbent dosage for fly ash agglomerates varied from 10 to 225 g/dm^3. The effect of the adsorbent dosage on the Cu(II) removal is presented in Fig. 4. The percentage removal of Cu(II) was increasing with adsorbent dosage. For the solution concentration 500 mg/dm^3 of Cu(II), the maximum uptake of Cu(II) by fly ash agglomerates was achieved for a minimal possible adsorbent-to-solute ration of 10 g/dm^3 and was 16.7 mg Cu(II)/g of adsorbent (Fig. 4a). The maximum removal of Cu(II) was c.a. 99% for maximal adsorbent-to-solute ratio 225 g/dm^3. For the solution concentration 1,000 mg/dm^3 of Cu(II), the maximum uptake of Cu(II) by fly ash agglomerates was achieved for a minimal possible adsorbent-to-solute ration of 10 g/dm^3 and was 43.82 mg Cu(II)/g of adsorbent (Fig. 4b). The maximum removal of Cu(II) was nearly 100% already from 90 g/dm^3 (adsorbent-to-solute ratio). From both figures (Figs. 4a and b), it can be noted that the adsorption capacity was found to decrease proportionally with an increase in the number of fly ash agglomerates. However, the Cu(II) removal effectiveness of fly ash agglomerates increasing with the increased adsorbent amount. It can be due to many vacant active sites onto fly ash agglomerates hence greater adsorption of Cu(II). As the initial concentration of Cu(II) is constant, Cu(II) ions can occupy only a certain number of active sites. For each concentration of ions, there is a corresponding dose of adsorbent at which adsorption equilibrium will be achieved.

3.2. Equilibrium time for the adsorption of Cu(II)

Fig. 5 shows the plot of Cu(II) adsorption capacity of fly ash agglomerates against contact time. It can be observed that the adsorption was rapid in the initial stages and increased with a rise in contact time up to 8 h at 25°C ± 1°C. After a time, there was no considerable change in the adsorption capacity of fly ash agglomerates. It could be attributed to a large number of vacant binding sites, which are available for adsorption during the initial stage, and after an increase in contact time, the occupation of the remaining vacant sites will be demanding due to the repulsive forces between the Cu(II) ions on the solid and the liquid phases [47]. As shown in Fig. 5, the removal of Cu(II) by fly ash agglomerates is a time-consuming process. The process was conducted for 24 h; however, the kinetics study revealed that the equilibrium was achieved after 8 h. The efficiency of Cu(II) removal was about 90%.

To evaluate the kinetics of the adsorption process, the Elovich, the PFO, and PSO models were tested to interpret the experimental data. The obtained kinetic model constants and R^2 values are shown in Table 3.

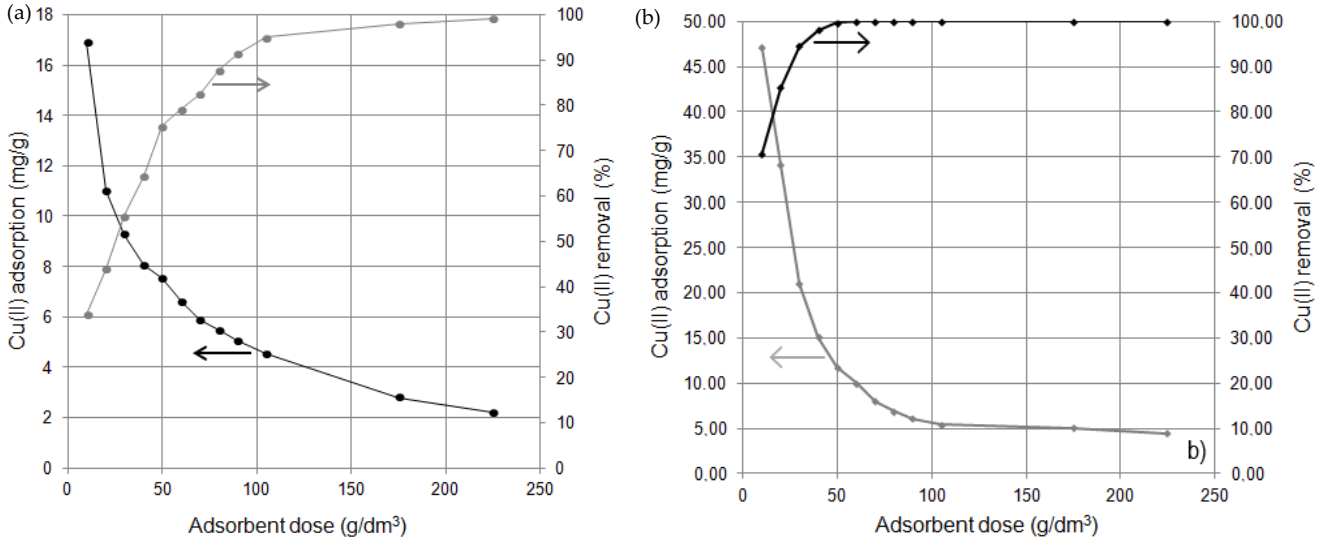

Fig. 4. Effect of adsorbent dose at (a) 500 mg/dm^3 and (b) 1,000 mg/dm3 of initial Cu(II) concentration.

The values of k_1 and Q_1, for the PFO model, were calculated using the slope and plots intercept of $\log(Q_1 - q_t)$ vs. t. PSO adsorption parameters Q_2 and k_2 in Eq. (7) were determined by plotting t/q_t vs. t. The correlation coefficient for the PSO kinetic model is exceptionally high ($R^2 = 0.999$), much higher than the correlation coefficients derived from the Elovich and PFO model fits. The excellent agreement between the experimental (Q_{exp}) and the calculated values of Q_2 demonstrate that the PSO model adequately describes the adsorption data obtained in the present study, and we can suggest that Cu(II) ions were adsorbed onto the fly ash agglomerates via chemical interaction. Similar trends have been reported for the adsorption of Cu(II) ions from aqueous solutions by other adsorbents [47,48,51,52]. The calculated average relative errors deviation (ARED) for kinetic models were added in Table 3. These values confirm that the PSO model is the best to describe the experimental data.

The adsorption mechanism also can be determined using the intra-particle model. As can be seen in Fig. 6, the adsorption of Cu(II) onto fly ash agglomerates is a three-stage process. The initial steeper section represents surface or film diffusion, the second linear section represents a gradual adsorption stage where intra-particle or pore diffusion is rate-limiting, and the third section is the final equilibrium stage. The values for k_{IP1} and k_{IP2} were calculated from the slope of each plot. Table 4 gives the values of these parameters (k_{IP1}, k_{IP2}, and b). The value of k_{IP2} is lesser than the value of k_{IP1} and suggested that the second step of Cu(II) adsorption had controlled the process in the present case because this step is slower than the first are. However, the calculated value of b (b ¹ 0) suggests that the intra-particle diffusion is not the sole rate-limiting step [13,30].

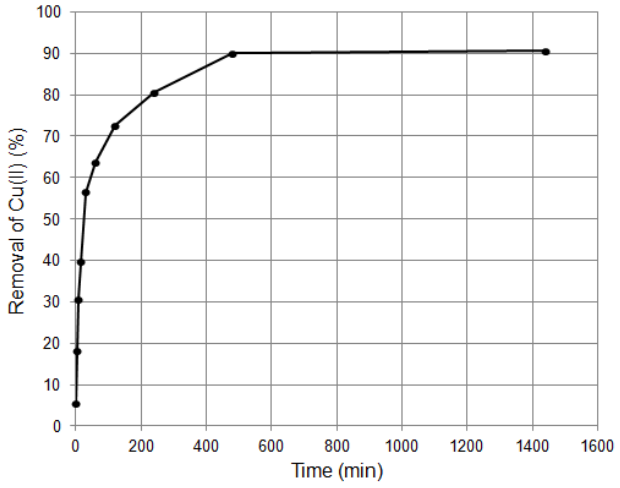

Fig. 5. The removal of Cu(II) by fly ash agglomerates (initial Cu(II) concentration: 1,000 mg/dm³; adsorbent dose: 50 g/dm³; pH 5.5; T = 25°C ± 1°C).

3.3. Effect of initial Cu(II) concentration

The initial concentration of metal ion is an essential variable at adsorption researchers. Therefore, the

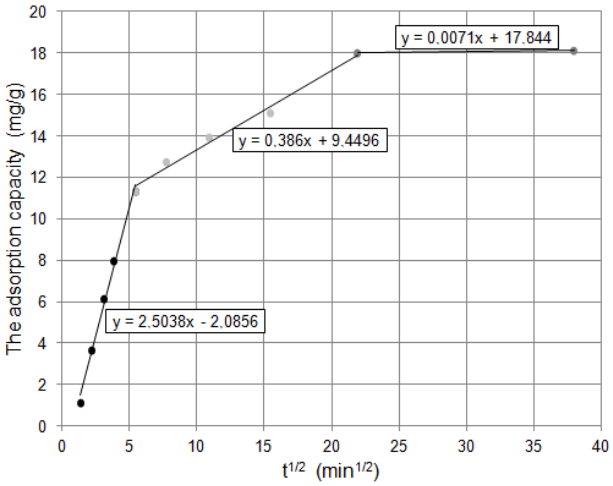

Fig. 6. Intraparticle diffusion plots for Cu(II) adsorption on fly ash agglomerates (initial Cu(II) concentration: 1,000 mg/dm³; adsorbent dose: 50 g/dm³; pH 5.5; T = 25°C ± 1°C).

Table 4
Constant parameters and correlation coefficients calculated for the intra-particle diffusion model (initial Cu(II) concentration: 1,000 mg/dm³, adsorbent dose: 50 g/dm³, pH 5.5, and T = 25°C ± 1°C)

Intra-particle diffusion	
k_{IP1} (mg/g min$^{1/2}$)	2.50
k_{IP2} (mg/g min$^{1/2}$)	0.386
b (mg/g)	9.45
R^2	0.9877

Table 3
Parameters of the kinetic models and the correlation coefficient

Q_{exp}	Elovich		PFO		PSO	
	α (g min²/mg)	1.63	k_1 (1/min)	$5.08 \cdot 10^{-3}$	k_2 (g/mg min)	$1.56 \cdot 10^{-3}$
	β (mg/g min)	0.375	Q_1 (mg/g)	9.62	Q_2 (mg/g)	16.80
18.13 mg/g	R^2	0.953	R^2	0.976	h (mg/g min)	0.441
					R^2	0.999
ARED	22.4%		46.9%		7.34%	

adsorption of Cu(II) onto fly ash agglomerates was studied at different initial Cu(II) concentrations ranging from 25 to 1,000 mg/dm^3 at pH 5.30 and 25°C ± 1°C. As shown in Fig. 7, while increasing the initial Cu(II) concentration, the adsorption amount (g/mg) is increased, and the adsorption percentage is decreasing. At lower concentrations, all Cu(II) ions in the solutions could interact with the active sites on the adsorbent, and thus the adsorption capacity was rapidly increased with increasing initial Cu(II) concentration. At higher concentrations, the adsorption capacity was nearly constant due to the saturation of the adsorption sites.

3.4. Adsorption isotherms

The Langmuir, Freundlich, and Dubinin–Radushkevich isotherm models were used to describe the equilibrium data in this study. The coefficient of determination (R^2) and the ARED were used to determine which isotherm model best describes experimental data. The calculated isotherm parameters for these models for the adsorption of Cu(II) onto fly ash agglomerates was shown in Table 5. Table 5, the calculated values of the coefficient of determination (R^2), and the ARED were shown. ARED can be calculated as follows [42]:

$$\text{ARED} = \frac{1}{N}\cdot\sum_{i=1}^{N}\left|\frac{\left(q_{\text{eq,cal}} - q_{\text{eq,exp}}\right)}{q_{\text{eq,exp}}}\right|\cdot 100\% \quad (15)$$

where N is the number of experiments, $q_{\text{eq,cal}}$ and $q_{\text{eq,exp}}$ are the equilibrium adsorption capacities of the adsorbent calculated and experimental, respectively (mg/g).

All equations fit the data reasonably well, but the best-fit was obtained with the Freundlich isotherm model ($R^2 > 0.99$). The fitting of experimental data by the Freundlich isotherm model is given in Fig. 8.

The Freundlich isotherm constants K_F and n are determined from the intercept and slope of a plot of $\log(q_{\text{eq}})$ vs. $\log(c_{\text{eq}})$. The Freundlich constant n has a value lying in the range of 1–10, which suggests that adsorption as favorable. The suitability of the Freundlich isotherm model indicates the heterogeneous surface of fly ash agglomerates and the multilayer adsorption of Cu(II) on this adsorbent.

The comparison of the four linearized Langmuir equations shows that the Langmuir-I give a higher value of correlation coefficient (R^2 = 0.9532) than that of the other three linearized equations. The values of parameters and R^2 shown in Table 5. From Table 5, it can be concluded that different linear Langmuir equations give non-identical values of parameters. The adsorption capacity of fly ash agglomerates was found to be 19.80 mg/g for Langmuir-I, and that of Langmuir II, III, and IV are 10.10, 12.30, and 14.90 mg/g, respectively. Thus, during linearization, errors in the computation of parameters may be responsible for the variation in the adsorption capacity (Q_L) and the Langmuir constant related to the free energy of adsorption (K_L) [42].

The use of DR isotherm allows the determination of the characteristic energy of adsorption. The adsorption energy (E) gives information about whether the adsorption mechanism is ion-exchange, chemisorptions, or physical adsorption. However, the D–R isotherm correlation coefficient is the lowest (R^2 = 0.6711) compared to the other three isotherm models (Table 5) and it is difficult to say that the calculated energy of adsorption will be reliable information.

Some authors found best-fitting of experimental data using Langmuir model of Cu(II) adsorption on different sorbents, such as activated carbon prepared from grape bagasse [48], activated and nonactivated date pits [49], zeolite derived from Indian fly ash [50], peat [51], natural clay [32], modified orange peel [52], multi-walled carbon nanotubes [33], and as well as various type of fly ash [12,13,31,53]. Freundlich isotherm model was reported to fit well for Cu(II) removal by rose waste biomass [54], iron oxide coated eggshell powder [55], banana, and orange peels [56].

The data obtained and their comparison with the information contained in the literature allow concluding, that the Langmuir model best describes the adsorption of Cu(II) on fly ash agglomerates. The maximum adsorption value is 19.80 mg/g (Table 5).

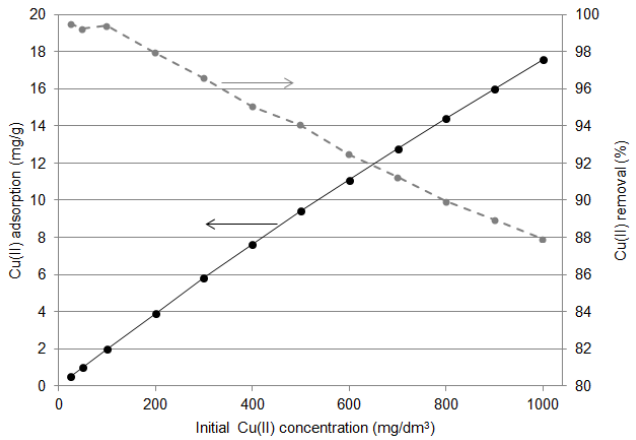

Fig. 7. Effect of initial Cu(II) concentration (initial Cu(II) concentration: 25–1,000 mg/dm^3; adsorbent dose: 50 g/dm^3; pH 5.5; T = 25°C ± 1°C).

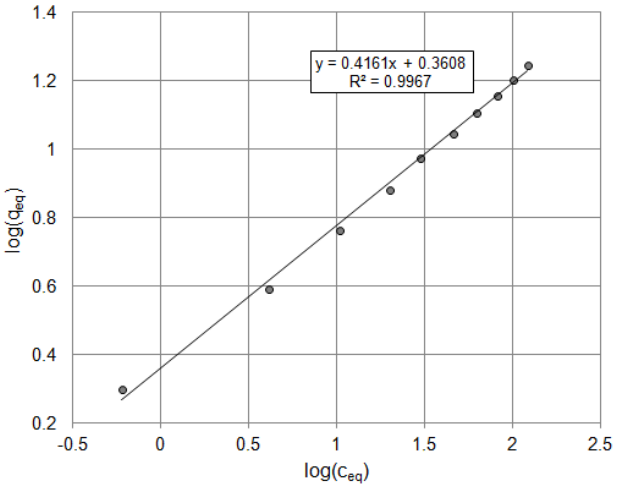

Fig. 8. Freundlich isotherm model of Cu(II) adsorption onto fly ash agglomerates (initial Cu(II) concentration: 25–1,000 mg/dm^3; adsorbent dose: 50 g/dm^3; pH 5.5; T = 25°C ± 1°C).

Table 5
Freundlich, Langmuir, Dubinin–Radushkevich isotherm parameters (initial Cu(II) concentration: 25–1,000 mg/dm^3, adsorbent dose: 50 g/dm^3, pH 5.5, and T = 25°C ± 1°C)

Isotherm	Parameters		Fitting	
Freundlich	n (–)	K_F (mg/g)	R^2 (–)	ARED (%)
	2.40	2.23	0.9934	6.43
Langmuir	Q_L (mg/g)	K_L (dm^3/mg)	R^2 (–)	ARED (%)
I	19.8	0.037	0.9532	13.1
II	10.1	0.395	0.8923	28.3
III	12.3	0.270	0.6514	29.7
IV	14.9	0.128	0.9032	14.9
Dubinin–Radushkevich	Q_{DR} (mg/g)	k_{DR} (mol^2/kJ^2)	R^2 (–)	ARED (%)
	9.91	3.79×10^{-9}	0.6711	43.7

3.5. Mathematical description of fixed-bed column studies

The loading behavior of Cu(II) removed from a fixed bed system/setup containing fly ash agglomerates media is shown by the breakthrough curve given in Fig. 9. The breakthrough curve is expressed using normalized concentrations and defined as a ratio of effluent Cu(II) concentration to the initial Cu(II) concentration (c/c_0) as a function of time (t) or volume of effluent (v_{eff}) for a given bed height (h). The volume of the effluent (v_{eff}) was determined using the following Eq. (16) [57,58]:

$$v_{eff} = Qt_{total} \tag{16}$$

The area under the breakthrough curve obtained by integrating the adsorbed concentration vs. the throughput volume plot can be used to find the total adsorbed Cu(II) quantity (the maximum column capacity). The adsorption capacity of the bed (q_0) can be calculated from Eq. (17) used by many authors for boron adsorption [23,24], chromium adsorption [59] and zinc adsorption [60]. This equation is given in the following form:

$$q_0 = \int_0^v c_{ads} \cdot \frac{dv}{m} \tag{17}$$

where c_{ads} is the initial Cu(II) concentration (c_0) is the effluent Cu(II) concentration (c_e).

The column capacity value of fly ash agglomerates (q_{exp}) is given in Table 7.

Adsorption in a fixed bed can be described by using two models: the Thomas and the Yoon–Nelson models. The experimental data of Cu(II) adsorption onto fly ash agglomerates packed in the column were fitted using these models. The Thomas equation and the Yoon–Nelson equation parameters for Cu(II) adsorption are shown in Table 6. The kinetic coefficient k_{Th} and the adsorption capacity of the column q_{Th} were calculated from a plot of $\ln((c_0/c_t) - 1)$ against t for Thomas model (Fig. 10). While the parameters k_{YN} and t were determined from a plot of $\ln(c_t/(c_0 - c_t))$ vs. t for Yoon–Nelson model (Fig. 11).

The maximum column capacity evaluated from the experiment (10.15 mg/g) is comparable with the value of the static uptake obtained from the batch experiments for the similar adsorbent-to-Cu(II) ratio (25.3 g/dm^3) (Fig. 4a). The calculated ARED from Eq. (15) were 3.94% and 7.09% for Thomas and Yoon–Nelson.

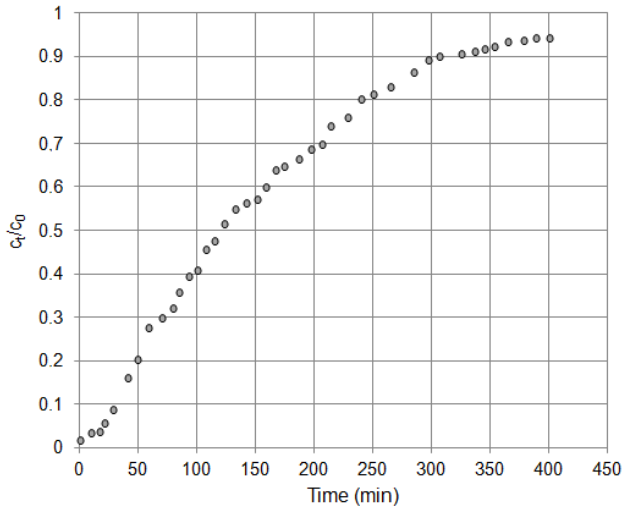

Fig. 9. Breakthrough curve for Cu(II) adsorption by fly ash agglomerates (particle size: 2.5–5.0 mm).

Some authors found the exceptional fit of experimental data using Thomas model of Cu(II) adsorption capacity on different materials, such as palm oil boiler mill fly ash (POFA) [57], chitosan immobilized on bentonite [58] or kenaf fibers [61] and biosorbent [62]. However, it is not easy to compare these adsorbents because each column capacity was determined in different process conditions such as different initial concentrations, bed height, or flow rate. It can be stated that the Thomas model is the most used model to describe the dynamics of adsorption.

After column studies, Cu(II) desorption experiments on fly ash agglomerates were carried out in static mode, that is, treatment of fly ash agglomerates with deionized water for 48 h. The Cu(II) concentration in eluates was below 1 mg/dm^3. Fly ash agglomerates used in this study are waste material. Therefore, the regeneration of adsorbent has not been examined.

Table 6
Parameters of the Thomas and Yoon–Nelson models

q_{exp}	Yoon–Nelson model		Thomas model	
10.15 mg/g	k_{YN} (1/min)	0.0132	k_{Th} (cm³/mg min)	2.45·× 10^{-5}
	τ_{YN} (min)	127.8	q_{Th} (mg/g)	10.55
	q_{YN} (mg/g)	9.43		
	R^2	0.9795	R^2	0.9781

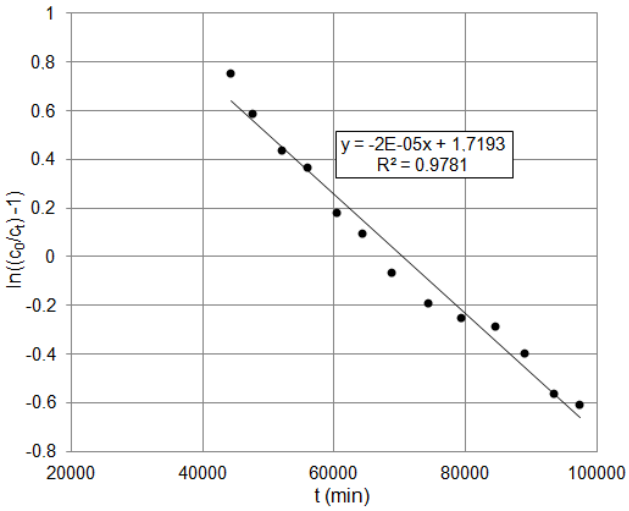

Fig. 10. The plot of $\ln((c_0/c_t)^{-1})$ vs. t according to Thomas model.

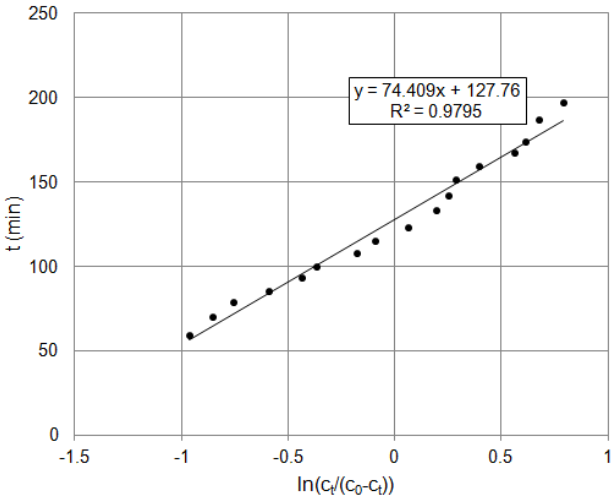

Fig. 11. The plot of t vs. $\ln((c_t/c_0–c_t))$ according to Yoon-Nelson model.

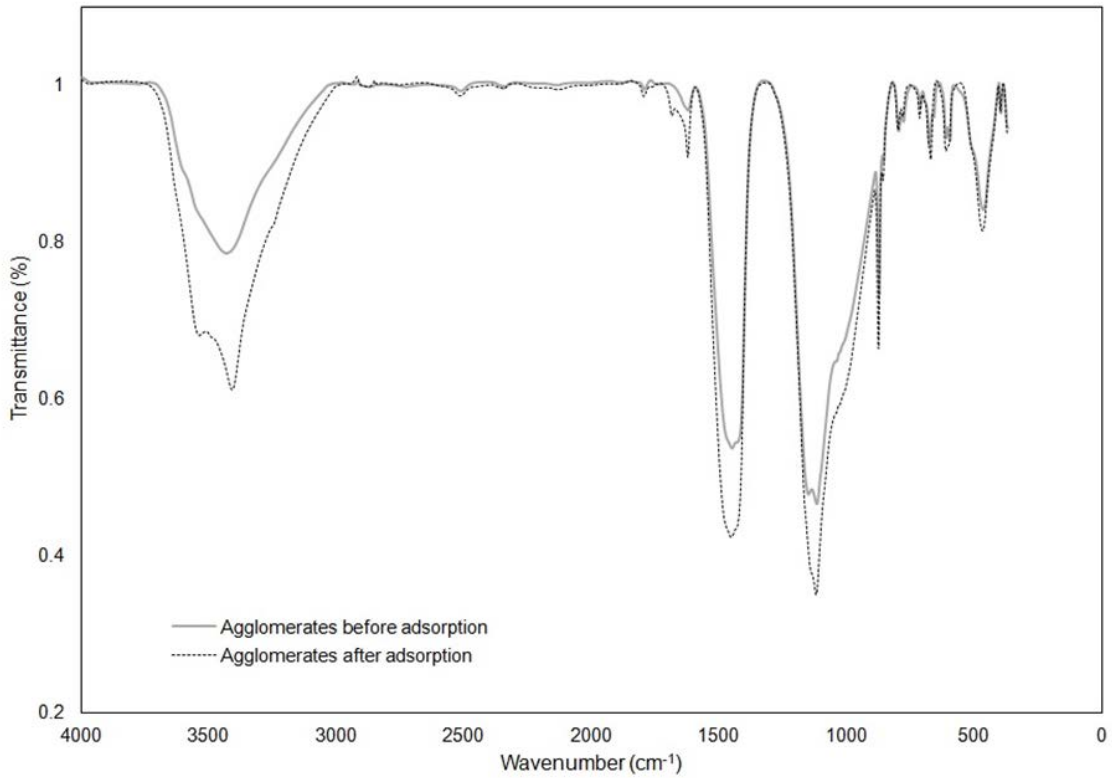

Fig. 12. FT-IR spectra obtained for fly ash agglomerates before and after Cu(II) adsorption.

3.6. FT-IR analysis

A detailed description of the FT-IR analysis of fly ash and fly ash agglomerates was presented in Polowczyk et al.s' [27] paper. The FT-IR spectra proved the presence of functional groups able to bind Cu(II) ions on fly ash agglomerates surface. Based on the FT-IR spectra (Fig. 12), the leading bands can be observed in the following ranges:

- 3,600–3,400 cm^{-1},
- 1,600 cm^{-1},
- 1,400–1,200 cm^{-1},
- 750–450 cm^{-1}.

The bands around 3,600–3,400 cm^{-1} and 1,600 cm^{-1} are associated with stretching and deformation vibrations of OH and H–O–H groups. The peak around 1,400 cm^{-1} might be ascribed to the presence of O–C–O stretching vibration in carbonate. The peak around 1,200 cm^{-1} indicates the presence of $–SO_4^{2-}$ species previously found in ettringite. The bands in the range of 750–450 cm^{-1} are caused by the in-plane bending vibration of Si–O–Si [63–68].

Comparing the FT-IR spectra of agglomerates before and after Cu(II) adsorption, significant changes can be observed (Fig. 12). Most of all, the appearance of changing in the bands of 3,600–3,400; 1,600; 1,400; and 1,200 cm^{-1}. The second characteristic difference is observed in the range of 750–450 cm^{-1}, where the C–S–H phase appeared. It can be assumed that bands' shifts are related to the Cu(II) bond by the respective groups. Increasing intensity of the bands at 1,200–1,100 cm^{-1} suggests the replacement of $–SO_4^{2-}$ ions originated from ettringite by Cu(II). The change in the chemical structure of this mineral can also be observed in the area 3,600–3,400 cm^{-1}, where the bands in unsaturated adsorbent increase after adsorption of Cu(II), indicating further changes. It can be assumed that the shifts in the bands are related to the Cu(II) bond by the respective groups. Chen et al. [69] and Giergiczny and Król [70] presented in their works that the C–S–H phase mostly controls the immobilization of heavy metal ions.

4. Conclusion

In the presented studies, the removal of Cu(II) from aqueous solutions was investigated using fly ash agglomerates (2.5–5.0 mm) in batch and column experiments. The results can be summarized as:

- The maximum adsorption capacity was found as 16.90 mg/g for initial Cu(II) concentration 500 mg/dm^3 and 44.90 mg/g for initial Cu(II) concentration 1,000 mg/dm^3.
- The maximum removal was achieved at about 99%.
- The kinetic study revealed that the adsorption kinetics of Cu(II) onto fly ash agglomerates obeys PSO model.
- Based on the IPD kinetic model, it can be stated that the Cu(II) adsorption onto fly ash agglomerates was a three-stage process.
- The experimental data were fitted well using the Freundlich isotherm, but the Langmuir model has also obtained high the correlation coefficient ($R^2 > 0.95$). The Dubinin–Radushkevich equation was not good for the description of Cu(II) adsorption on fly ash agglomerates.
- The column capacity value was obtained by graphical integration as 10.15 mg/g for the adsorbent-to-solute ration of 25.3 g/dm^3. The experimental data were described by using Thomas and Yoon–Nelson models.
- Agglomerated fly ash can be an effective adsorbent for removing of Cu(II) from aqueous solutions. The fly ash agglomerates are economic competitiveness resulting from the simplicity of gathering these adsorbents comparing to expensive and commercial solutions. Moreover, the proposed application may be the complex response for disposal of wastes created in electric plants.

Acknowledgment

The work was financed by a subsidy for the Wroclaw University of Science and Technology No. 8201003902.

Symbols

b	—	Film thickness, mg/g
c_0	—	Initial Cu(II) concentrations, mg/dm^3
c_{eq}	—	Equilibrium Cu(II) concentrations, mg/dm^3
c_{eq}	—	Equilibrium Cu(II) concentration in the solution, mg/dm^3
c_t	—	Effluent Cu(II) concentration, mg/dm^3
E	—	Low free energy of adsorption, J/mol
F	—	Volumetric flow rate, dm^3/min
h	—	Initial adsorption rate, mg/g min
k_1	—	Rate constant of the PFO equation, 1/min
k_2	—	Rate constant of the PSO equation, g/mg min
k_{DR}	—	Constant related to the adsorption energy, mol^2/kJ^2
K_F	—	Freundlich constant related to the adsorption capacity of adsorbent, mg/g
k_{IP}	—	Intra-particle diffusion model rate constant, mg/g $min^{1/2}$
K_L	—	Langmuir constant related to the free energy of adsorption, dm^3/g
k_{Th}	—	Thomas rate constant, dm^3/mg min
k_{YN}	—	Rate constant, 1/min
m	—	Amount of adsorbent used, g
n	—	Freundlich exponent indicating the adsorption intensity, –
q	—	Amount of adsorption, mg/g
Q_1	—	Amount of soluted adsorbate adsorbed at equilibrium, mg/g
Q_2	—	Amount of adsorption equilibrium, mg/g
Q_{DR}	—	Theoretical saturation capacity, mg/g
q_{eq}	—	Equilibrium adsorption capacities of the adsorbent, mg/g
Q_L	—	Monolayer adsorption capacities of the adsorbent, mg/g
q_t	—	Adsorption capacity at time, mg/g
q_{Th}	—	Adsorption capacities of the adsorbent, mg/g
R	—	Gas constant, J/mol K
t	—	Time, min
T	—	Absolute temperature, K
t_{total}	—	Total time of flow till exhaust, min

V — Volume of the solution, dm^3
v_{eff} — Volume of effluent, dm^3
α — Initial sorption rate, g min^2/mg
β — Parameter of Elovich model, mg/g min
ε — Polanyi potential, J/mol
τ — Time required for 50% adsorbate breakthrough, min

References

[1] L. Trakal, R. Šigut, H. Šillerová, D. Faturíková, M. Komárek, Copper removal from aqueous solution using biochar: effect of chemical activation, Arabian J. Chem., 7 (2014) 43–52.
[2] A. Baran, J. Antonkiewicz, Phytotoxicity and extractability of heavy metals from industrial waste, Environ. Prot. Eng., 43 (2017) 143–155.
[3] M.N. Chileshe, S. Syampungani, E.S. Festin, M. Tigabu, A. Daneshvar, P.C. Odén, Physico-chemical characteristics and heavy metal concentrations of copper mine wastes in Zambia: implications for pollution risk and restoration, Eur. J. For. Res., 17 (2015) 622–631.
[4] M.R. Awual, T. Yaita, S.A. El-Safty, H. Shiwaku, S. Suzuki, Y. Okamoto, Copper(II) ions capturing from water using ligand modified a new type mesoporous adsorbent, Chem. Eng. J., 221 (2013) 322–330.
[5] S.A. Al-Saydeh, M.H. El-Naas, S.J. Zaidi, Copper removal from industrial wastewater: a comprehensive review, J. Ind. Eng. Chem., 56 (2017) 35–44.
[6] M.R. Awual, M. Ismael, M.D. Khaleque, T. Yaita, Ultra-trace copper(II) detection and removal from wastewater using novel meso-adsorbent, J. Ind. Eng. Chem., 20 (2014) 2332–2340.
[7] M. Araya, M. Olivares, F. Pizarro, Copper in human health, Int. J. Environ. Health, 1 (2007) 608–620.
[8] A. Shahbazi, H. Younesi, A. Badiei, Batch and fixed-bed column adsorption of Cu(II), Pb(II) and Cd(II) from aqueous solution onto functionalised SBA-15 mesoporous silica, Can. J. Chem. Eng., 91 (2013) 739–750.
[9] J. Thilagan, V. Adichakkravarthy, K. Rajsekran, C. Raja, Continuous fixed bed column adsorption of copper(II) ions from aqueous solution by calcium carbonate, Int. J. Eng. Tech. Res., 4 (2015) 413–418.
[10] M. Goyal, V.K. Rattan, D. Aggarwal, R.C. Bansal, Removal of copper from aqueous solutions by adsorption on activated carbons, Colloids Surf., A, 190 (2001) 229–238.
[11] F. Bouhamed, Z. Elouear, J. Bouzid, Adsorptive removal of copper(II) from aqueous solutions on activated carbon prepared from Tunisian date stones: equilibrium, kinetics and thermodynamics, J. Taiwan Inst. Chem. Eng., 43 (2012) 741–749.
[12] L. Darmayanti, S. Notodarmodjo, E. Damanhuri, Removal of copper(II) ions in aqueous solutions by sorption onto fly ash, J. Eng. Technol. Sci., 49 (2017) 546–559.
[13] E. Sočo, J. Kalembkiewicz, Removal of copper(II) and zinc(II) ions from aqueous solution by chemical treatment of coal fly ash, Croat. Chem. Acta, 88 (2015) 267–279.
[14] T. Hsu, C. Yu, C. Yeh, Adsorption of Cu^{2+} from water using raw and modified coal fly ashes, Fuel, 87 (2008) 1355–1359.
[15] M. Ahmaruzzaman, A review on the utilization of fly ash, Prog. Energy Combust. Sci., 36 (2010) 327–363.
[16] V.C. Pandey, N. Singh, Impact of fly ash incorporation in soil systems, Agric. Ecosyst. Environ., 136 (2010) 16–27.
[17] H. Cho, D. Oh, K. Kim, A study on removal characteristics of heavy metals from aqueous solution by fly ash, J. Hazard. Mater., B127 (2005) 187–195.
[18] J. Ulatowska, I. Polowczyk, W. Sawiński, A. Bastrzyk, T. Koźlecki, Z. Sadowski, Use of fly ash and fly ash agglomerates for As(III) adsorption from aqueous solution, Pol. J. Chem. Technol., 16 (2014) 21–27.
[19] A.D. Papandreou, C.J. Stournaras, D. Panias, I. Paspaliaris, Adsorption of Pb(II), Zn(II) and Cr(III) on coal fly ash porous pellets, Miner. Eng., 24 (2011) 1495–1501.
[20] J. Aguilar-Carrillo, F. Garrido, L. Barrios, M.T. Garcia-Gonzalez, Sorption of As, Cd and Tl as influenced by industrial by–products applied to an acidic soil: equilibrium and kinetics experiments, Chemosphere, 65 (2006) 2377–2387.
[21] J. Wang, X. Teng, H. Wang, H. Ban, Characterizing the metal adsorption capability of a class F coal fly ash, J. Environ. Sci. Technol., 38 (2004) 6710–6715.
[22] V.K. Gupta, I. Ali, Utilisation of bagasse fly ash (a sugar industry waste) for the removal of copper and zinc from wastewater, Sep. Purif. Technol., 18 (2000) 131–140.
[23] I. Polowczyk, J. Ulatowska, T. Koźlecki, A. Bastrzyk, W. Sawiński, Studies on removal of boron from aqueous solution by fly ash agglomerates, Desalination, 310 (2013) 93–101.
[24] N. Öztürk, D. Kavak, Adsorption of boron from aqueous solutions using fly ash: batch and column studies, J. Hazard. Mater., B127 (2005) 81–88.
[25] F. Ferrero, Dye removal from aqueous solution using coal fly ash for continuous flow adsorption, Clean Technol. Environ. Policy, 17 (2015) 1907–1915.
[26] U.B. Deshannavar, B.G. Katageri, M. El-Harbawi, A. Parab, K. Acharya, Fly ash as an adsorbent for the removal of reactive blue 25 dye from aqueous solutions: optimization, kinetic and isotherm investigations, Proc. Est. Acad. Sci., 66 (2017) 300–308.
[27] I. Polowczyk, J. Ulatowska, A. Bastrzyk, T. Koźlecki, P. Cyganowski, Research on Agglomeration of Fly Ash as a Method of Improving Its Utilization, J. Parker, Ed., Fly Ash: Properties, Analysis and Performance, Nova Science Publisher's Inc., Hauppauge, NY, 2017, pp. 177–193.
[28] A.D. Papandreou, C.J. Stournaras, D. Panias, Copper and cadmium adsorption on pellets made from fried coal fly ash, J. Hazard. Mater., 148 (2007) 538–547.
[29] N. Priyantha, L.B.L. Lim, S. Wickramasooriya, C.H. Ing, Adsorption behavior of Cu(II) ions on thermally-treated peat of Muthurajawela, Sri Lanka, Water Desal. Res. J., 3 (2019) 1–15.
[30] M.L.F.A. DeCastro, M.L.B. Abad, D.A.G. Sumalinog, R.R.M. Abarca, P. Paoprasert, M.D.G. De Luna, Adsorption of Methylene Blue dye and Cu(II) ions on EDTA-modified bentonite: Isotherm, kinetic and thermodynamic studies, Sustainable Environ. Res., 28 (2018) 197–205.
[31] P. Wu, Y. Tang, Z. Cai, Dual role of coal fly ash in copper ion adsorption followed by thermal stabilization in a spinel solid solution, RSC Adv., 8 (2018) 8805–8812.
[32] A.T. Sdiri, T. Higashi, F. Jamoussi, Adsorption of copper and zinc onto natural clay in single and binary systems, Int. J. Environ. Sci. Technol., 11 (2014) 1081–1092.
[33] I. Mobasherpour, E. Salahi, M. Ebrahimi, Thermodynamics and kinetics of adsorption of Cu(II) from aqueous solutions onto multi-walled carbon nanotubes, J. Saudi Chem. Soc., 18 (2014) 792–801.
[34] Z. Aksu, İ.A. İşoğlu, Removal of copper(II) ions from aqueous solution by biosorption onto agricultural waste sugar beet pulp, Process Biochem., 40 (2005) 3031–3044.
[35] M. Harja, G. Buema, D. Sutiman, C. Munteanu, D. Bucur, Low cost adsorbents obtained from ash for copper removal, Korean J. Chem. Eng., 29 (2012) 1735–1744.
[36] M.J.D. Low, Kinetics of chemisorptions of gases on solids, Chem. Rev., 60 (1960) 267–312.
[37] Y.S. Ho, J.C.Y. Ng, G. McKay, Kinetics of pollutant sorption by biosorbents: review, Sep. Purif. Technol., 29 (2000) 189–232.
[38] S. Lagergren, Zur theorie der Sogenannten adsorption geloster stoffe, Kungl. Svens. Vetenskapsakad. Handl., 24 (1898) 1–24.
[39] Y.S. Ho, G. McKay, Pseudo-second order model for sorption processes, Process Biochem., 34 (1999) 451–465.
[40] H.M.F. Freundlich, Über die Adsorption Lösungen, Z. Phys. Chem., 57 (1906) 385–470.
[41] I. Langmuir, The constitution and fundamental properties of solids and liquids, J. Am. Chem. Soc., 38 (1916) 2221–2295.
[42] B. Subramanyam, A. Das, Linearised and non-linearised isotherm models optimization analysis by error functions and statistical means, J. Environ. Health Sci. Eng., 12 (2014) 1–6.
[43] M.M. Dubinin, L.V. Radushkevich, The equation of the characteristics curve of activated charcoal, Proc. Acad. Sci. USSR, 55 (1947) 331–333.

[44] H.C. Thomas, Heterogeneous ion exchange in a flowing system, J. Am. Chem. Soc., 66 (1944) 1664–1666.
[45] K.H. Chu, Fixed bed sorption: setting the record straight on the Bohart–Adams and Thomas models, J. Hazard. Mater., 177 (2010) 1006–1012.
[46] Y.H. Yoon, J.H. Nelson, Application of gas adsorption kinetics I. A theoretical model for respirator cartage service life, Am. Ind. Hyg. Assoc. J., 45 (1984) 509–516.
[47] M. Arshadi, M.J. Amini, S. Mousavi, Kinetic, equilibrium and thermodynamic investigations of Ni(II), Cd(II), Cu(II) and Co(II) adsorption on barley straw ash, Water Resour. Ind., 6 (2014) 1–17.
[48] H. Demiral, C. Gűngőr, Adsorption of copper(II) from aqueous solutions on activated carbon prepared from grape bagasse, J. Cleaner Prod., 124 (2016) 103–113.
[49] N.M. Hilal, I.A. Ahmed, R.E. El-Sayed, Activated and nonactivated date pits adsorbents for the removal of copper(II) and cadmium(II) from aqueous solutions, ISRN Phys. Chem., 2012 (2012) 1–11.
[50] T. Mishra, S.K. Tiwari, Studies on sorption properties of zeolite derived from Indian fly ash, J. Hazard. Mater., 137 (2006) 299–303.
[51] T. Zehra, L.B.L. Lim, N. Priyantha, Characterization of peat samples collected from Brunei Darussalam and their evaluation as potential adsorbents for Cu(II) removal from aqueous solution, Desal. Water Treat., 57 (2016) 20889–20903.
[52] N. Feng, X. Guo, S. Liang, Adsorption study of copper(II) by chemically modified orange peel, J. Hazard. Mater., 164 (2009) 1286–1292.
[53] T. Benzaoui, A. Selatnia, D. Djabali, Adsorption of copper(II) ions from aqueous solution using bottom ash of expired drugs incineration, Adsorpt. Sci. Technol., 36 (2017) 114–129.
[54] A.R. Iftikhar, H.N. Bhatti, M.A. Hanif, R. Nadeem, Kinetic and thermodynamic aspects of Cu(II) and Cr(III) removal from aqueous solutions using rose waste biomass, J. Hazard. Mater., 161 (2009) 941–947.
[55] R. Ahmad, R. Kumar, S. Haseeb, Adsorption of Cu^{2+} from aqueous solution onto iron oxide coated eggshell powder: evaluation of equilibrium, isotherms, kinetics, and regeneration capacity, Arabian J. Chem., 5 (2012) 353–359.
[56] A. Annadurai, R.S. Juang, D.J. Lee, Adsorption of heavy metals from water using banana and orange peels, Water Sci. Technol., 47 (2002) 185–190.
[57] A.S.A. Aziz, L.A. Manaf, H.C. Man, N.S. Kumar, Column dynamic studies and breakthrough curve analysis for Cd(II) and Cu(II) ions adsorption onto palm oil boiler mill fly ash (POFA), Environ. Sci. Pollut. Res. Int., 21 (2014) 7996–8005.
[58] C.M. Futalan, C.C. Kan, M.L. Dalida, C. Pascua, M.W. Wan, Fixed-bed column studies on the removal of copper using chitosan immobilized on bentonite, Carbohydr. Polym., 82 (2011) 697–704.
[59] P. Suksabye, P. thiravetyan, W. Nakbanpote, Column study of chromium(VI) adsorption from electroplating industry by coconut coir pith, J. Hazard. Mater., 160 (2008) 56–62.
[60] A. Saravanan, P.S. Kumar, M. Yaswanthraj, Modeling and analysis of paced-bed column for effective removal of zinc from aqueous solution using dual surface-modified biomass, Part. Sci. Technol., 36 (2018) 934–944.
[61] C.M. Hasfalina, R.Z. Maryam, C.A. Luqman, M. Rashid, Adsorption of copper(II) from aqueous medium in fixed-bed column by kenaf fibres, APCBEE Procedia, 3 (2012) 255–263.
[62] A. Abdolali, H.H. Ngo, W. Guo, J.L. Zhou, J. Zhang, S. Liang, S.W. Chang, D.D. Nguyen, Y. Liu, Application of a breakthrough biosorbent for removing heavy metals from synthetic and real wastewaters in lab-scale continuous fixed-bed column, Bioresour. Technol., 229 (2017) 78–87.
[63] S.J. Barnett, D.E. Macphee, E.E. Lachowski, N.J. Crammond, XRD, EDX and IR analysis of solid solutions between thaumasite and ettringite, Cem. Concr. Res., 32 (2002) 719–730.
[64] P. Chindaprasirt, C. Jaturapitakkul, W. Chalee, U. Rattanasak, Comparative study on the characteristics of fly ash and bottom ash geopolymers, Waste Manage., 29 (2009) 539–543.
[65] S. Coussy, D. Paktune, J. Rose, M. Benzaazoua, Arsenic speciation in cemented paste backfills and synthetic calcium-silicate-hydrates, Miner. Eng., 39 (2012) 51–61.
[66] I. García-Lodeiro, A. Palomo, A. Fernández-Jiménez, Alkali-aggregate reaction in activated fly ash systems, Cem. Concr. Res., 37 (2007) 175–183.
[67] D. Gastaldi, F. Canonico, E. Boccaleri, Ettringite and calcium sulfoaluminate cement investigation of water content by near-infrared spectroscopy, J. Mater. Sci., 44 (2009) 5788–5794.
[68] P. Yu, R.J. Kirkpatrick, B. Poe, P.F. McMillan, X. Cong, Structure of calcium silicate hydrate (C-S-H): near-, mid- and far- infrared spectroscopy, J. Am. Ceram. Soc., 82 (1999) 742–748.
[69] Q.Y. Chen, M. Tyrer, C.D. Hills, X.M. Yang, P. Carey, Immobilization of heavy metal in cement-based solidification/stabilization: a review, Waste Manage., 29 (2009) 390–403.
[70] Z. Giergiczny, A. Król, Immobilization of heavy metals (Pb, Cu, Cr, Zn, Cd, Mn) in the mineral additions containing concrete composites, J. Hazard. Mater., 160 (2008) 247–255.